J. Fluid Mech. (2007), *vol.* 592, *pp.* 367–392.
doi:10.1017/S0022112007008488 Printed in the United Kingdom

Sound generated by aerodynamic sources near a deformable body, with application to voiced speech

M. S. HOWE[1]† AND R. S. McGOWAN[2]

[1]Boston University, College of Engineering 110 Cummington Street, Boston, MA 02215, USA
[2]CReSS LLC, 1 Seaborn Place, Lexington, MA 02420, USA

(Received 7 January 2007 and in revised form 12 July 2007)

An analysis is made of sound generation by aerodynamic sources near an acoustically compact body (or compact surface feature on a large boundary) that can deform in an arbitrary manner. It is shown how such problems can be investigated by simple extension of the compact Green's function used in the treatment of compact rigid bodies. It is known that this method can furnish rapid and accurate predictions of sound generated by flows with extensive, non-compact distributions of sources in cases where a numerical treatment requires at best tens or hundreds of hours of CPU time. Illustrative applications are made to study (i) the sound generated by a nominally rigid circular lamina of time-dependent radius held in an irrotational mean stream, and (ii) the production of voiced speech by vorticity interacting with a simple model of the vocal folds. In case (ii), it appears that predictions are represented well by a quasi-static approximation that permits the particular results of this paper and previous investigations to be generalized to arbitrarily configured folds.

1. Introduction

Unsteady vorticity in a nominally homogeneous compressible fluid is a source of *aerodynamic* sound (Lighthill 1952; Howe 1998, 2003). In low-Mach-number flows, it is often permissible to regard the motion as *homentropic*, and to neglect the convection of sound by the flow. Lighthill's (1952) equation for the production of sound then assumes the form

$$\left(\frac{1}{c_o^2}\frac{\partial^2}{\partial t^2} - \nabla^2\right) B = \mathrm{div}(\boldsymbol{\omega}\wedge\boldsymbol{v}), \tag{1.1}$$

where c_o is the mean speed of sound, which can be regarded as uniform and constant, and B is the *total enthalpy* defined in homentropic flow by

$$B = \int \frac{\mathrm{d}p}{\rho} + \tfrac{1}{2}v^2, \tag{1.2}$$

where $\boldsymbol{v}$ is the velocity, $\boldsymbol{\omega} = \mathrm{curl}\,\boldsymbol{v}$ the vorticity, and $\rho \equiv \rho(p)$ is the density.

In the absence of vorticity and moving boundaries, Bernoulli's equation implies that B is constant throughout the flow, and may be assumed to vanish. Equation (1.1)

† Author to whom correspondence should be addressed: mshowe@bu.edu

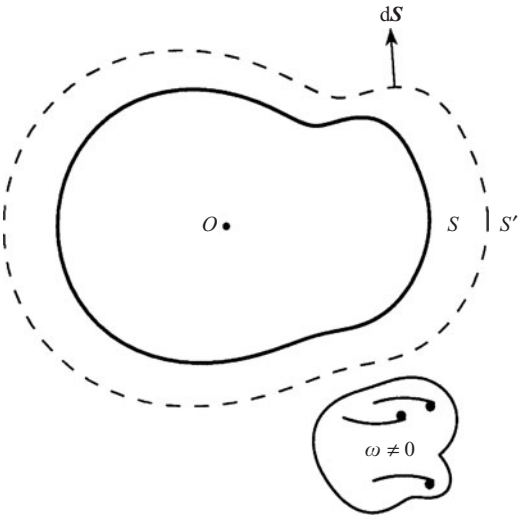

FIGURE 1. Vortex sources adjacent to a moving solid body S with enclosing control surface $S'(t)$.

implies that fluctuations in B propagate as sound away from regions of unsteady vorticity within which the divergence of the Lamb vector $\boldsymbol{\omega} \wedge \boldsymbol{v}$ represents the effective aeroacoustic source. The equation usefully determines the sound when $\mathrm{div}(\boldsymbol{\omega} \wedge \boldsymbol{v})$ is prescribed or has been determined by preliminary analysis. In the exterior propagation zone, the motion is irrotational and described by a velocity potential $\varphi(\boldsymbol{x}, t)$, where Bernoulli's equation implies that $B = -\partial\varphi/\partial t$. The equations of motion may be linearized in the far field, where the acoustic pressure is determined by $p \approx -\rho_o \partial\varphi/\partial t = \rho_o B$.

The efficiency with which aerodynamic sound is produced is strongly influenced by the presence of solid boundaries in the source flow (Curle 1955; Crighton & Leppington 1971; Crighton 1975*a*, *b*). In an unbounded medium, a vortex source is equivalent to a quadrupole for which the amplitude of the acoustic pressure $p \sim O(\rho_o v^2 M^2)$, where $M \sim v/c_o \ll 1$ is a characteristic Mach number. When M is small, the amplitude is increased by a factor $\sim 1/M$ for sources in the vicinity of a solid boundary S, say (figure 1), because unsteady forces induced on S by the vorticity are generally equivalent to more efficient dipoles for which $p \sim O(\rho_o v^2 M)$.

Dipoles are particularly important in noise-control problems involving moving boundaries S (Beranek & Vér 1992; Howe 1998; Howe *et al.* 2006). Predictions in such cases usually depend on the introduction of an acoustic Green's function $G(\boldsymbol{x}, \boldsymbol{y}, t, \tau)$ satisfying

$$\left(\frac{1}{c_o^2}\frac{\partial^2}{\partial\tau^2} - \frac{\partial^2}{\partial y_j^2}\right) G = \delta(\boldsymbol{x} - \boldsymbol{y})\delta(t - \tau), \quad G = 0 \text{ for } \tau > t, \tag{1.3}$$

together with suitable conditions on a moving material control surface $S' \equiv S'(t)$ within the fluid that just encloses the physical boundary S.

The usual requirement is that the normal derivatives $\partial G/\partial x_n$, $\partial G/\partial y_n$ should vanish respectively for $\boldsymbol{x}$ and $\boldsymbol{y}$ on S'. The application of Green's theorem and the radiation condition to (1.1) and (1.3) then enable the solution of (1.1) to be expressed

in the form (Baker & Copson 1969; Landau & Lifshitz 1987; Crighton *et al.* 1992; Howe 1998)

$$B(\boldsymbol{x},t) = -\oint_{S'(\tau)} G(\boldsymbol{x},\boldsymbol{y},t,\tau)\frac{\partial B}{\partial y_j}(\boldsymbol{y},\tau)\,\mathrm{d}S_j(\boldsymbol{y})\,\mathrm{d}\tau + \int G(\boldsymbol{x},\boldsymbol{y},t,\tau)\frac{\partial}{\partial y_j}(\boldsymbol{\omega}\wedge\boldsymbol{v})_j(\boldsymbol{y},\tau)\,\mathrm{d}^3\boldsymbol{y}\,\mathrm{d}\tau, \tag{1.4}$$

where the integration is taken over all values of the 'retarded time' $-\infty < \tau < +\infty$, the surface integral is over $S'(\tau)$ (with surface element $\mathrm{d}\boldsymbol{S}$ directed into the fluid 'outside' $S'(\tau)$), and the volume integral is over the external region of the fluid occupied by the vortex sources.

Integration by parts permits the final integral on the right-hand side to be replaced by

$$-\oint_{S'(\tau)} G(\boldsymbol{x},\boldsymbol{y},t,\tau)(\boldsymbol{\omega}\wedge\boldsymbol{v})_j(\boldsymbol{y},\tau)\,\mathrm{d}\boldsymbol{S}_j(\boldsymbol{y})\,\mathrm{d}\tau - \int(\boldsymbol{\omega}\wedge\boldsymbol{v})_j(\boldsymbol{y},\tau)\frac{\partial G}{\partial y_j}(\boldsymbol{x},\boldsymbol{y},t,\tau)\,\mathrm{d}^3\boldsymbol{y}\,\mathrm{d}\tau. \tag{1.5}$$

When this is substituted into (1.4), the remaining surface integrals are simplified as follows. Write the momentum equation in Crocco's form (Howe 1998)

$$\frac{\partial \boldsymbol{v}}{\partial t} + \nabla B = -\boldsymbol{\omega}\wedge\boldsymbol{v} - \nu\,\mathrm{curl}\,\boldsymbol{\omega}, \tag{1.6}$$

where ν is the kinematic viscosity. Viscosity can usually be ignored in 'noisy' high-Reynolds-number flows. For this reason, the contribution to (1.6) from the bulk viscosity has been discarded, because its effect is small everywhere. However, the shear viscosity is responsible for possibly significant frictional forces on S and is therefore retained, but in doing so it is also assumed at low Mach numbers that $\nu =$ constant.

Thus, taking account of these remarks and the relations (1.5) and (1.6), and taking the limit in which the control surface S' shrinks down onto S, (1.4) is found to reduce to

$$\begin{aligned} B(\boldsymbol{x},t) = &-\int(\boldsymbol{\omega}\wedge\boldsymbol{v})_j(\boldsymbol{y},\tau)\frac{\partial G}{\partial y_j}(\boldsymbol{x},\boldsymbol{y},t,\tau)\,\mathrm{d}^3\boldsymbol{y}\,\mathrm{d}\tau \\ &+\nu\oint_{S(\tau)}\boldsymbol{\omega}(\boldsymbol{y},\tau)\wedge\frac{\partial G}{\partial \boldsymbol{y}}(\boldsymbol{x},\boldsymbol{y},t,\tau)\cdot\mathrm{d}\boldsymbol{S}(\boldsymbol{y})\,\mathrm{d}\tau \\ &+\oint_{S(\tau)} G(\boldsymbol{x},\boldsymbol{y},t,\tau)\frac{\partial v_j}{\partial \tau}(\boldsymbol{y},\tau)\,\mathrm{d}\boldsymbol{S}_j(\boldsymbol{y})\,\mathrm{d}\tau, \end{aligned} \tag{1.7}$$

where $B(\boldsymbol{x},t)\approx p(\boldsymbol{x},t)/\rho_o$ in the linear acoustic region, far from the sources.

The first integral represents the sound generated by vortex sources within the fluid-including the influence of the solid surface S, whose presence determines the functional form of $G(\boldsymbol{x},\boldsymbol{y},t,\tau)$. The surface integral involving ν supplies the contribution from frictional forces on S. The final term accounts for an unsteady normal velocity on S: the limit $S'\to S$ therefore implies that sound is produced by a distribution of surface monopoles represented by unsteady motions of S.

In an important class of practical problems the boundary S, or some prominent geometrical feature of S, is acoustically compact, that is, small compared to the wavelength of the sound produced by the motion. For rigid bodies, the dominant source is then of dipole type and the sound can be computed accurately from (1.7) when S is stationary or in uniform or accelerated rectilinear motion by replacing $G(\boldsymbol{x},\boldsymbol{y},t,\tau)$ by its compact approximation (Howe 1975, 1998).

The purpose of this paper is to show how the method of compact Green's function can be applied to compact bodies (or compact surface elements) in arbitrary low-Mach-number motion, including situations where the shape and volume of the body change with time. The general case of free-space radiation in three dimensions is discussed in § 2. It is illustrated (§ 3) by the example of sound generation by a stationary, nominally rigid, disk-shaped lamina of time-dependent radius due to the action of *Coanda* edge-flow suction forces in the presence of a steady mean irrotational flow, for which the validity of our conclusions is easily checked by alternative means.

Extension is made in § 4 to study sound generation in a duct of compact cross-section by sources in the vicinity of a deformable contraction. The compact Green's function for this configuration is used in §§ 5 and 6 to investigate the aeroacoustics of 'voiced speech' (Fant 1960; Flanagan 1972; Stevens 1998), that is, the mechanism of sound generation by the vocal folds of the larynx. The subject has been investigated numerically (Zhao *et al.* 2002; Hofmans *et al.* 2003; Duncan, Zhai & Scherer 2006) by modelling the vocal tract as a uniform waveguide divided into two sections at the glottis, the opening of variable width between the two vocal folds. 'Voicing' occurs when high pressure in the lungs opens the glottis producing a mean flow and inducing quasi-periodic vibrations of the folds. The vibration is accompanied by vortex shedding, and the generated sound can be attributed to a combination of vortex-induced dipoles (associated with the drag on the folds) and a monopole governed by small volumetric changes of the flexing vocal fold structure.

2. Compact deformable bodies

2.1. *The compact Green's function*

Consider the case in which the surface S of figure 1 is acoustically compact and is either stationary or executing small-amplitude translational oscillations. The leading-order approximation to the radiation field (1.7), i.e. the solution that is correct to terms of monopole and dipole order, can be evaluated by means of the following compact approximation for $G(\boldsymbol{x}, \boldsymbol{y}, t, \tau)$ (Howe 1975, 1998, 2003):

$$G(\boldsymbol{x}, \boldsymbol{y}, t, \tau) = \frac{1}{4\pi|\boldsymbol{X}-\boldsymbol{Y}|}\delta\left(t-\tau-\frac{|\boldsymbol{X}-\boldsymbol{Y}|}{c_o}\right), \tag{2.1}$$

where $\boldsymbol{X}$, $\boldsymbol{Y}$ are, respectively, representations in terms of $\boldsymbol{x}$ and $\boldsymbol{y}$ of the Kirchhoff vector

$$\boldsymbol{X} = \boldsymbol{x} - \boldsymbol{\varphi}^*(\boldsymbol{x}), \quad \boldsymbol{Y} = \boldsymbol{y} - \boldsymbol{\varphi}^*(\boldsymbol{y}). \tag{2.2}$$

The jth component φ_j^* is defined to equal the velocity potential (vanishing at infinity) of the incompressible flow that would be produced by rigid-body motion of S at unit speed in the j-direction. Therefore, the vector components $X_j(\boldsymbol{x})$ and $Y_j(\boldsymbol{y})$ can be interpreted as the velocity potentials of incompressible flow past the stationary S having unit speed in the j-direction at large distances from S. The representation (2.1) is applicable provided at least one of the points $\boldsymbol{x}$, $\boldsymbol{y}$ lies in the acoustic far field of S (see Howe 1998 for further discussion).

The compact approximation is expressed in the form (2.1) in order that it shall reduce to the free-space Green's function (which determines the solution (1.7) in the absence of the boundary S) when $\boldsymbol{X}$ and $\boldsymbol{Y}$ reduce, respectively, to $\boldsymbol{x}$ and $\boldsymbol{y}$. In applications, (2.1) must first be expanded correct to dipole order to furnish explicit predictions. Thus, when the origin O and the source point $\boldsymbol{y}$ are both near S, the

observation point $\boldsymbol{x}$ must be taken to be in the acoustic far field where $|\boldsymbol{X}| \approx |\boldsymbol{x}| \gg |\boldsymbol{Y}|$, and

$$G(\boldsymbol{x}, \boldsymbol{y}, t, \tau) \approx \frac{1}{4\pi|\boldsymbol{x}|}\delta\left(t - \tau - \frac{|\boldsymbol{x}|}{c_o}\right) + \frac{x_i Y_i}{4\pi c_o|\boldsymbol{x}|^2}\delta'\left(t - \tau - \frac{|\boldsymbol{x}|}{c_o}\right), \quad |\boldsymbol{x}| \to \infty, \tag{2.3}$$

where the prime denotes differentiation with respect to t. The first term in this formula does not depend on the source position $\boldsymbol{y}$, and determines the monopole component of the sound; the second represents the dipole. The question of which of these terms dominates the far field depends on the properties of the source terms in the integrands of (1.7).

2.2. *Compact body in arbitrary, deformable motion*

The approximation (2.1) is also applicable to problems involving a compact body S in arbitrary, deformable motion. This is readily verified by a simple modification of the 'Rayleigh matching' argument used in the proof of (2.1) (Howe 1998), and is similar to that given below in § 4 for sound generation in a deformable wave guide. In applications, account must be taken of the time-dependence of the Kirchhoff vectors $X_j \equiv X_j(\boldsymbol{x}, t)$, $Y_j \equiv Y_j(\boldsymbol{y}, \tau)$, each of which represents a uniform potential flow past S defined by its instantaneous position and shape.

The procedure is illustrated well by consideration of the final surface integral in the general solution (1.7). The monopole component of the sound is governed by the first term on the right-hand side of (2.3), which gives

$$\frac{1}{4\pi|\boldsymbol{x}|}\oint_{S(\tau)}\delta\left(t - \tau - \frac{|\boldsymbol{x}|}{c_o}\right)\frac{\partial v_j}{\partial \tau}(\boldsymbol{y}, \tau)\,\mathrm{d}S_j(\boldsymbol{y})\,\mathrm{d}\tau = \frac{1}{4\pi|\boldsymbol{x}|}\left[\frac{\partial}{\partial t}\oint_S \boldsymbol{v}\cdot\mathrm{d}\boldsymbol{S} - \oint_S (\mathrm{div}\,\boldsymbol{v})\boldsymbol{v}\cdot\mathrm{d}\boldsymbol{S}\right]$$

$$\approx \frac{1}{4\pi|\boldsymbol{x}|}\left[\frac{\partial}{\partial t}\oint_S \boldsymbol{v}\cdot\mathrm{d}\boldsymbol{S}\right], \tag{2.4}$$

where the square brackets denote evaluation of the contents at the retarded time $t - |\boldsymbol{x}|/c_o$, and the divergence term is dropped because it is $O(M^2) \ll 1$ relative to the first in the low-Mach-number source region.

Similarly, the second term in (2.3) supplies the dipole

$$\frac{x_i}{4\pi c_o|\boldsymbol{x}|^2}\oint_{S(\tau)}\delta'\left(t - \tau - \frac{|\boldsymbol{x}|}{c_o}\right)Y_i(\boldsymbol{y}, \tau)\frac{\partial v_j}{\partial \tau}(\boldsymbol{y}, \tau)\,\mathrm{d}S_j(\boldsymbol{y})\,\mathrm{d}\tau$$

$$= \frac{x_j}{4\pi c_o|\boldsymbol{x}|^2}\frac{\partial}{\partial t}\left[\frac{\partial}{\partial t}\oint_S Y_j\boldsymbol{v}\cdot\mathrm{d}\boldsymbol{S} - \oint_S\left(\frac{\partial Y_j}{\partial t} + \mathrm{div}\,(Y_j\boldsymbol{v})\right)\boldsymbol{v}\cdot\mathrm{d}\boldsymbol{S}\right]$$

$$\approx \frac{x_j}{4\pi c_o|\boldsymbol{x}|^2}\frac{\partial}{\partial t}\left[\frac{\partial}{\partial t}\oint_S Y_j\boldsymbol{v}\cdot\mathrm{d}\boldsymbol{S} - \oint_S \frac{DY_j}{Dt}\boldsymbol{v}\cdot\mathrm{d}\boldsymbol{S}\right]. \tag{2.5}$$

The remaining integrals in (1.7) involve only the term in $Y_j(\boldsymbol{y}, \tau)$ of (2.3). Making the substitution and combining with (2.4) and (2.5) we obtain the following representation of the sound in the far field, where $B = p/\rho_o$,

$$p(\boldsymbol{x}, t) \approx \frac{\rho_o}{4\pi|\boldsymbol{x}|}\left[\frac{\partial}{\partial t}\oint_S \boldsymbol{v}\cdot\mathrm{d}\boldsymbol{S}\right] + \frac{\rho_o x_j}{4\pi c_o|\boldsymbol{x}|^2}\frac{\partial}{\partial t}\left[\frac{\partial}{\partial t}\oint_S Y_j\boldsymbol{v}\cdot\mathrm{d}\boldsymbol{S} - \oint_S \frac{\mathrm{D}Y_j}{\mathrm{D}t}\boldsymbol{v}\cdot\mathrm{d}\boldsymbol{S}\right.$$

$$\left. + \nu\oint_S \boldsymbol{\omega}\wedge\frac{\partial Y_j}{\partial \boldsymbol{y}}\cdot\mathrm{d}\boldsymbol{S}(\boldsymbol{y}) - \int(\boldsymbol{\omega}\wedge\boldsymbol{v})\cdot\frac{\partial Y_j}{\partial \boldsymbol{y}}\,\mathrm{d}^3\boldsymbol{y}\right], \quad |\boldsymbol{x}| \to \infty. \tag{2.6}$$

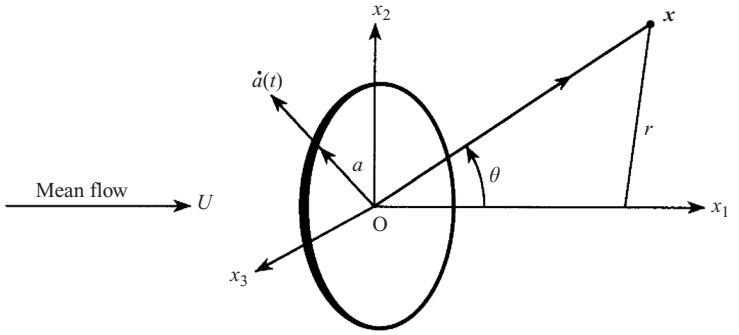

FIGURE 2. Generation of sound by a thin disk of time-dependent radius $a(t)$ placed broadside-on to a uniform irrotational mean stream.

This approximation is correct to dipole order in a multipole expansion of the far field. The first term on the right represents omnidirectional monopole radiation produced by volumetric pulsations of the body S. The remaining terms are dipoles and are nominally smaller by a factor $\sim O(M)$, but they become the dominant part of the acoustic field when the volume of the deforming solid is either constant or changes by only a small amount.

3. Sound produced by a disk of time-dependent radius

Consider an acoustically compact rigid disk of infinitesimal thickness whose radius $a = a(t)$ is oscillating about some mean value with arbitrary amplitude. The disk is placed broadside-on to a uniform mean stream of speed U, where $M = U/c_o$ is small. Dipole sound is produced as a result of vortex shedding from the disk and because of the fluctuations in disk size. However, there is no monopole radiation because the disk is a deformable body whose volume does not change. The mechanism of sound production shares some similarities with that of voiced speech considered in §§ 5 and 6. In particular, it involves a change in the geometrical size of the radiating structure with no change of volume, or at least only a very small change in volume in the case of the vocal folds. For the present, we wish to examine the influence on the sound of the variable radius and therefore confine attention to the case of an ideal fluid where vortex shedding does not occur and the mean flow is irrotational. Such a flow is singular at the edge of the disk where the infinite velocity produces the suction force required to turn the flow around the sharp corner – a 'Coanda effect'. It will be seen that it is the rate of working of the unsteady component of this Coanda edge force that is responsible for the generation of sound.

Take the origin of coordinates $\boldsymbol{x} = (x_1, x_2, x_3)$ at the fixed location of the centre of the disk, with the x_1 axis normal to the disk and in the direction of the mean flow (figure 2). Then the mean flow velocity is $U\nabla X_1(\boldsymbol{x}, t)$ where X_1 is the component in the x_1 direction of the Kirchhoff vector which, when the coordinate axes are orientated as in figure 2, is given by

$$\left.\begin{aligned} X_1 &= x_1 + \frac{2a\,\mathrm{sgn}(x_1)}{\pi}\int_0^\infty \left(\frac{\sin(\xi a)}{\xi a} - \cos(\xi a)\right)\frac{\exp(-\xi|x_1|)J_0(\xi r)\,\mathrm{d}\xi}{\xi}, \\ r &= \sqrt{x_2^2 + x_3^2}, \\ X_2 &= x_2, \quad X_3 = x_3, \end{aligned}\right\} \tag{3.1}$$

where $a = a(t)$ and J_0 is the Bessel function of order zero.

For future reference we note the following asymptotic approximations

$$X_1 \sim \frac{2\sqrt{2a}}{\pi}\mathrm{Re}\left(\exp(\mathrm{i}\pi/4)\sqrt{z-\mathrm{i}a}\right), \quad z \sim \mathrm{i}a, \quad z = x_1 + \mathrm{i}r, \tag{3.2a}$$

$$X_1 \sim x_1\left(1 + \frac{2a^3}{3\pi|\boldsymbol{x}|^3}\right), \quad |\boldsymbol{x}| \gg a, \tag{3.2b}$$

$$X_1 = \pm\frac{2\sqrt{a^2-r^2}}{\pi}, \quad x_1 \to \pm 0, \ r < a. \tag{3.2c}$$

The streamline pattern defined by $X_1(\boldsymbol{x}, t)$ is qualitatively similar to that for potential flow in the normal direction past a thin strip, as illustrated in figure 3.6.4 of Howe (2003).

We use (2.6) to calculate the sound in the far field of the disk. Because the volume of the disk always vanishes and $\boldsymbol{\omega} = \boldsymbol{0}$, only the first two surface integrals in the dipole term can possibly make a non-trivial contribution. However, the normal component of velocity vanishes on the front and back faces of the disk (where $\boldsymbol{v}\cdot\mathrm{d}\boldsymbol{S} \equiv 0$). This means that any contribution to the integrals must be a consequence of singular behaviour of the integrands at the edge of the disk. The potential flow edge behaviour of (3.2*a*) indicates, in fact, that

$$p(\boldsymbol{x}, t) \approx -\frac{\rho_o x_j}{4\pi c_o|\boldsymbol{x}|^2}\frac{\partial}{\partial t}\left[\oint_S \frac{\mathrm{D}Y_j}{\mathrm{D}t}\boldsymbol{v}\cdot\mathrm{d}\boldsymbol{S}\right] = -\frac{\rho_o x_1}{4\pi c_o|\boldsymbol{x}|^2}\frac{\partial}{\partial t}\left[\oint_S U(\nabla Y_1)^2\boldsymbol{v}\cdot\mathrm{d}\boldsymbol{S}\right] \tag{3.3}$$

because $(\nabla Y_1)^2 \sim O(1/|z-\mathrm{i}a|)$ near the edge. The entire contribution to the last integral is from the immediate vicinity of the edge, where the normal component of velocity is $\dot{a}(t) = \mathrm{d}a/\mathrm{d}t$ (see figure 2). It is evaluated by the method described by Batchelor (1967, equation (6.5.4)) for calculating suction force at a sharp edge, which yields

$$p(\boldsymbol{x}, t) \approx -\frac{2\rho_o M\cos\theta}{3\pi|\boldsymbol{x}|}\left[\frac{\mathrm{d}^2}{\mathrm{d}t^2}(a^3)\right]_{t-|\boldsymbol{x}|/c_o}, \quad |\boldsymbol{x}| \to \infty, \tag{3.4}$$

where θ is the angle shown in figure 2 between the radiation direction and the positive x_1 axis. This is a characteristic dipole field whose amplitude and frequency are determined by the time rate of change of the disk radius. Observe that there is no requirement that the overall amplitude of the radial variations should be small, although the frequency should be small enough to ensure that the disk remains acoustically compact.

The validity of (3.4) can be confirmed by the following alternative analysis, based on the far-field approximation (3.2*b*), which shows that the velocity potential in the hydrodynamic far field of the disk is given to dipole order by

$$\varphi_0 = UX_1 \sim Ux_1\left(1 + \frac{2a^3}{3\pi|\boldsymbol{x}|^3}\right), \quad |\boldsymbol{x}| \gg a. \tag{3.5}$$

The pressure $p(\boldsymbol{x}, t)$ is therefore

$$p(\boldsymbol{x}, t) = -\rho_o\frac{\partial\varphi_0}{\partial t} \approx -\frac{2\rho_o U}{3\pi}\frac{\partial}{\partial t}\left(\frac{x_1 a^3}{|\boldsymbol{x}|^3}\right) \equiv \frac{2\rho_o U}{3\pi}\frac{\partial^2}{\partial x_1\partial t}\left(\frac{a^3(t)}{|\boldsymbol{x}|}\right), \quad |\boldsymbol{x}| \gg a. \tag{3.6}$$

This formula is extended into the acoustic far field by replacing $a(t)$ by $a(t-|\boldsymbol{x}|/c_o)$ (Howe 2003, § 5.6), to obtain

$$p(\boldsymbol{x},t) \approx \frac{2\rho_o U}{3\pi}\frac{\partial^2}{\partial x_1 \partial t}\left(\frac{a^3(t-|\boldsymbol{x}|/c_o)}{|\boldsymbol{x}|}\right) \sim -\frac{2\rho_o M x_1}{3\pi|\boldsymbol{x}|^2}\left[\frac{\mathrm{d}^2}{\mathrm{d}t^2}(a^3)\right]_{t-|\boldsymbol{x}|/c_o}, \quad |\boldsymbol{x}| \to \infty, \tag{3.7}$$

which is equivalent to (3.4).

Alternatively, using $\varphi_0 = UX_1$ and the surface relation (3.2c), we find that the unsteady drag (in the $+x_1$ direction) experienced by the disk is

$$F(t) = 2\pi\int_0^{a(t)}\left[\rho_o\frac{\partial\varphi_0}{\partial t}\right]_{x_1=-0}^{+0} r\,\mathrm{d}r = 8\rho_o U a\dot{a}\int_0^a \frac{r\,\mathrm{d}r}{\sqrt{a^2-r^2}} = \frac{8\rho_o U}{3}\frac{\mathrm{d}}{\mathrm{d}t}(a^3).$$

The radiation produced by this force is given by (Curle 1955; Howe 2003, § 5.4)

$$p(\boldsymbol{x},t) \approx \frac{1}{4\pi|\boldsymbol{x}|}\frac{\partial F}{\partial x_1}\left(t-\frac{|\boldsymbol{x}|}{c_o}\right) \sim -\frac{x_1}{4\pi c_o|\boldsymbol{x}|^2}\left[\frac{\mathrm{d}F}{\mathrm{d}t}\right]_{t-|\boldsymbol{x}|/c_o}, \quad |\boldsymbol{x}| \to \infty, \tag{3.8}$$

which is again equivalent to (3.4).

The acoustic energy flux should equal the rate of working of the suction force at the edge of the disk. To verify this we first calculate the mean acoustic power radiating through the surface S_∞ of a large sphere of radius R_∞ centred on the disk, namely

$$\Pi = \oint_{S_\infty}\frac{\langle p^2\rangle\,\mathrm{d}S}{\rho_o c_o} = \frac{16\rho_o M^2}{27\pi c_o}\left\langle\left|\frac{\mathrm{d}^2}{\mathrm{d}t^2}(a^3)\right|^2\right\rangle, \tag{3.9}$$

where the angle brackets denote a time average and (3.4) has been used for p.

Next, using (3.4) and the far-field relation $p = -\rho_o\partial\varphi/\partial t$, it follows by expanding in powers of the 'compactness operator'

$$\frac{|\boldsymbol{x}|}{c_o}\frac{\partial}{\partial t}$$

that

$$\varphi - \varphi_0 = -\frac{U}{3\pi c_o^2}\frac{x_1}{|\boldsymbol{x}|}\frac{\mathrm{d}^2}{\mathrm{d}t^2}(a^3) + \frac{2Ux_1}{9\pi c_o^3}\frac{\mathrm{d}^3}{\mathrm{d}t^3}(a^3) + \cdots s, \quad |\boldsymbol{x}| \gg a, \tag{3.10}$$

where $a^3 \equiv a^3(t)$ and φ_0 is the the incompressible component (3.5) of the potential. Near the disk $\varphi = U\nabla X_1 + \varphi'$, where φ' is the hydrodynamic near-field representation of the terms on the right-hand side of (3.10). Now, the mean rate of working of the suction force is

$$\left\langle\oint_S -\tfrac{1}{2}\rho_o(\nabla\varphi)^2\boldsymbol{v}\cdot\mathrm{d}\boldsymbol{S}\right\rangle \approx \left\langle -\rho_o U\oint_S(\nabla X_1\cdot\nabla\varphi')\boldsymbol{v}\cdot\mathrm{d}\boldsymbol{S}\right\rangle.$$

However, in the near-field representation of φ', only the term corresponding to the second of the terms on the right-hand side of (3.10) (which represents a uniform flow in the x_1 direction) gives a non-zero average, namely

$$-\frac{2\rho_o M^2}{9\pi c_o}\left\langle\frac{\mathrm{d}^3}{\mathrm{d}t^3}(a^3)\oint_S(\nabla X_1)^2\boldsymbol{v}\cdot\mathrm{d}\boldsymbol{S}\right\rangle = -\frac{2\rho_o M^2}{9\pi c_o}\left\langle\frac{\mathrm{d}^3}{\mathrm{d}t^3}(a^3)\times\frac{8}{3}\frac{\mathrm{d}}{\mathrm{d}t}(a^3)\right\rangle$$
$$= \frac{16\rho_o M^2}{27\pi c_o}\left\langle\left|\frac{\mathrm{d}^2}{\mathrm{d}t^2}(a^3)\right|^2\right\rangle,$$

which is just equal to the acoustic power (3.9).

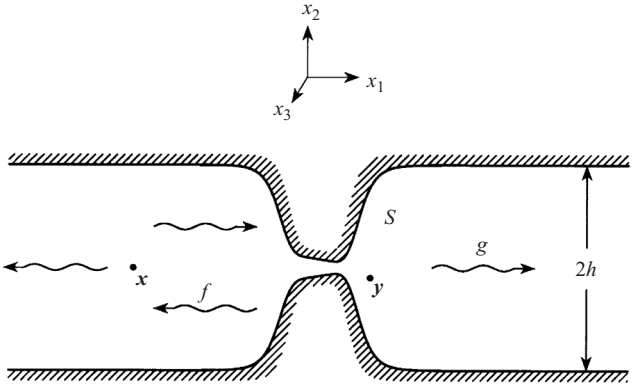

FIGURE 3. Schematic configuration of a duct with a localized, deformable contraction. The wave directions are for the direct compact Green's function G^D calculated for $|\boldsymbol{x}| \gg h$ and for $\boldsymbol{y}$ in the immediate neighbourhood of the contraction.

4. Duct with a deformable contraction

We now turn our attention to the problem illustrated schematically in figure 3 of sound production by sources in a nominally uniform duct with a compact deformable contraction. It is assumed that the duct is acoustically rigid everywhere except in the neighbourhood of the contraction, and that the characteristic frequencies are small enough to admit only of plane wave propagation in the duct. In what follows the configuration of figure 3 will be applied to study 'voiced speech': the deformable contraction will be used to model the vocal folds and glottis of the human larynx. First, it is necessary to determine the Green's function defined as in § 2, with vanishing normal derivative on the duct walls and on the instantaneous surface $S(\boldsymbol{x}, t)$ of the contraction.

Acoustic sources in the speech problem are at points $\boldsymbol{y}$ close to the contraction, and it is required to determine the sound radiated to distant points $\boldsymbol{x}$ in the uniform sections of the duct. To study the mechanism of sound production, it is unnecessary to account for reflections from the distant ends of the duct, which can therefore be taken to be infinite in both directions. There is no limitation on the cross-sectional shape of the uniform section of the duct, but numerical predictions are given in § 5 for a rectangular duct of span ℓ_3 and 'vertical' height $2h$ (where $\ell_3 \sim O(2h)$, see figure 3), and it will be convenient to frame the discussion in terms of this geometry.

4.1. *Green's function*

Take the coordinate origin at a point on the duct axis at the 'centre' of the contraction, with the x_1 axis parallel to the duct axis and directed to the right in figure 3. Consider first the case where the observer at $\boldsymbol{x}$ is in the distant acoustic region to the left-hand side of the contraction (x_1 large and negative, as in the figure). Green's function $G(\boldsymbol{x}, \boldsymbol{y}, t, \tau)$ defined by (1.3) propagates as a function of $(\boldsymbol{y}, \tau)$ as an 'advanced potential' that collapses into the singularity at $(\boldsymbol{x}, t)$ at time $\tau = t$ and vanishes for $\tau > t$. Its calculation is simplified, however, by the observation that $G(\boldsymbol{x}, \boldsymbol{y}, t, \tau)$ is the adjoint of the solution G^D, say, of the direct problem of the production of sound by a point source at $(\boldsymbol{x}, \tau)$ when the sound is regarded as propagating as a function of $(\boldsymbol{y}, t)$.

Let G_0^D be the solution of the direct problem when the contraction is absent, for a uniform duct. Then G^D can be determined by examining the interaction of G_0^D with

the contraction. The calculation is particularly straightforward when G^D is required for applications at low frequencies, when only plane waves can propagate in the uniform duct, because only the plane wave component of G_0^D is then relevant, namely

$$G_0^D = \frac{c_o}{2\mathscr{A}} H\left(t - \tau - \frac{|x_1 - y_1|}{c_o}\right), \tag{4.1}$$

where $\mathscr{A} = 2h\ell_3$ is the cross-sectional area of the uniform section of the duct, and H is the Heaviside step function.

The combination of G_0^D and of waves produced when the disturbance (4.1) impinges on the contraction determines G^D in the approximation in which the contraction is compact. In this limit, the functional forms of G^D at points $\boldsymbol{y}$ in the acoustic far field of the contraction and within the contraction zone can be derived by matching alternative representations of G^D in two regions of overlap on either side of the contraction, where both representations are applicable.

4.2. *The compact approximation*

Suppose first that $x_1 < 0$ and is in the acoustic far field (see figure 3). When y_1 is to the right of the source, but several duct diameters to the left of the contraction ($x_1 < y_1 \ll 0$), G^D consists of the wave (4.1) travelling towards the contraction and a plane wave f reflected at the contraction, i.e.

$$G^D = \frac{c_o}{2\mathscr{A}} H\left([t] - \tau - \frac{y_1}{c_o}\right) + f\left([t] - \tau + \frac{y_1}{c_o}\right) \quad \text{where} \quad [t] = t + \frac{x_1}{c_o}. \tag{4.2}$$

The disturbance to the right of the contraction consists of the outgoing wave

$$G^D = g\left([t] - \tau - \frac{y_1}{c_o}\right), \quad y_1 \gg 0. \tag{4.3}$$

Near the contraction, the long-wavelength motion can be regarded as incompressible, and we can put

$$G^D = \mathscr{F}^D(t) + \mathscr{G}^D(t) Y_1(\boldsymbol{y}, t), \quad \boldsymbol{y} \sim O(h), \tag{4.4}$$

where $\mathscr{F}^D$, $\mathscr{G}^D$ are auxiliary functions and Y_1 is the (one-dimensional) Kirchhoff vector for the contraction at time t, defined such that $\partial Y_1/\partial y_1 \to 1$ as $y_1 \to \pm\infty$. It is a solution of Laplace's equation satisfying $\partial Y_1/\partial y_n = 0$ on the deformable surface $S(t)$ of the contraction, and can be normalized such that

$$Y_1 \sim y_1 \pm \frac{\ell(t)}{2}, \quad y_1 \to \pm\infty, \tag{4.5}$$

where $\ell(t)$ is the time-dependent Rayleigh 'end correction' of the contraction (Rayleigh 1945), given by

$$\ell(t) = \int_{-\infty}^{\infty} \left(\frac{\partial Y_1}{\partial y_1}(\boldsymbol{y}, t) - 1\right) \mathrm{d}y_1. \tag{4.6}$$

The integration is along any path parallel to the duct axis passing through the contraction.

The four unknown functions f, g, $\mathscr{F}$, $\mathscr{G}$ are found by expanding in powers of y_1/c_o and matching the formulae (4.2), (4.4) and (4.3), (4.4) correct to $O(y_1)$ in the respective common hydrodynamic regions of overlap $-c_o/\omega \ll y_1 \ll -h$ and $h \ll y_1 \ll c_o/\omega$ to the left and right of the contraction, where $\omega \sim \partial/\partial t$ is a characteristic frequency. This

procedure supplies the four equations

$$\left.\begin{aligned} \frac{c_o}{2\mathscr{A}} H([t]-\tau) + f([t]-\tau) &= \mathscr{F}^D(t) - \tfrac{1}{2}(\mathscr{G}^D\ell)(t), \\ \frac{-c_o}{2\mathscr{A}} \delta([t]-\tau) + f'([t]-\tau) &= c_o \mathscr{G}^D(t), \\ g([t]-\tau) &= \mathscr{F}^D(t) + \tfrac{1}{2}(\mathscr{G}^D\ell)(t), \\ g'([t]-\tau) &= -c_o \mathscr{G}^D(t), \end{aligned}\right\} \tag{4.7}$$

where a prime denotes differentiation with respect to the argument. By eliminating f and g, the equations determining $\mathscr{F}^D$ and $\mathscr{G}^D$ are obtained in the form

$$\frac{\partial \mathscr{F}^D}{\partial t} = \frac{c_o}{2\mathscr{A}} \delta([t]-\tau), \quad \frac{\partial}{\partial t}\left(\mathscr{G}^D\ell\right) + 2c_o\mathscr{G}^D = -\frac{c_o}{\mathscr{A}} \delta([t]-\tau). \tag{4.8}$$

Reverting now to the adjoint problem, we find for $\boldsymbol{y}$ in the vicinity of the contraction that

$$G(\boldsymbol{x}, \boldsymbol{y}, t, \tau) \approx \mathscr{F}(\tau) + \mathscr{G}(\tau) Y_1(\boldsymbol{y}, \tau), \tag{4.9}$$

where $\mathscr{F}(\tau)$, $\mathscr{G}(\tau)$ are solutions of the adjoints of (4.8):

$$\frac{\partial \mathscr{F}}{\partial \tau} = -\frac{c_o}{2\mathscr{A}} \delta([t]-\tau), \quad \ell(\tau)\frac{\partial \mathscr{G}}{\partial \tau} - 2c_o\mathscr{G} = \frac{c_o}{\mathscr{A}} \delta([t]-\tau). \tag{4.10}$$

A similar set of equations is obtained when $x_1 > 0$, in the duct to the right of the contraction. In both cases their solutions determine the following explicit form of (4.9) (for $\boldsymbol{y} \sim h$ in the vicinity of the contraction)

$$\begin{aligned} G(\boldsymbol{x}, \boldsymbol{y}, t, \tau) \approx \frac{c_o}{2\mathscr{A}} H([t]-\tau) + \frac{c_o \operatorname{sgn}(x_1) Y_1(\boldsymbol{y}, \tau)}{\ell([t])\mathscr{A}} H([t]-\tau) \\ \times \exp\left(-\int_\tau^{[t]} \frac{2c_o \mathrm{d}\xi}{\ell(\xi)}\right), \quad \boldsymbol{y} \sim O(h), \end{aligned} \tag{4.11}$$

where $[t] = t - |x_1|/c_o$.

The end correction ℓ typically exceeds the duct width $2h$, and becomes very large when the minimum distance between opposite walls of the contraction is small. The exponential function in the second term of (4.11) decreases rapidly when the acoustic travel distance $c_o([t]-\tau)$ exceeds ℓ, which provides a time scale for acoustically compact transients. In many applications of (4.11), however, transients are unimportant, inasmuch as typical compact sources near the contraction are effectively unchanged over time intervals $\sim \ell/c_o$. We can then use the relation

$$\lim_{\epsilon \to +0} \frac{1}{\epsilon} H(-x) \mathrm{e}^{x/\epsilon} = \delta(x)$$

to reduce (4.11) to the more conventional form

$$\begin{aligned} G(\boldsymbol{x}, \boldsymbol{y}, t, \tau) &\approx \frac{c_o}{2\mathscr{A}} \left\{ H\left(t - \tau - \frac{|x_1|}{c_o}\right) + \frac{\operatorname{sgn}(x_1)}{c_o} Y_1(\boldsymbol{y}, \tau) \delta\left(t - \tau - \frac{|x_1|}{c_o}\right) \right\} \\ &\approx \frac{c_o}{2\mathscr{A}} H\left(t - \tau - \frac{|x_1 - Y_1|}{c_o}\right), \quad |x_1| \to \infty. \end{aligned} \tag{4.12}$$

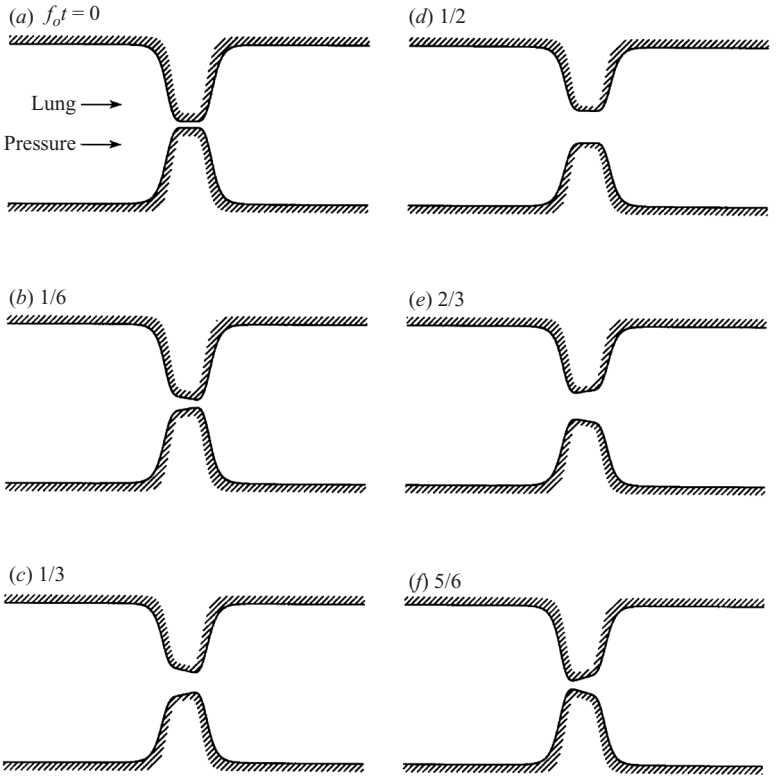

FIGURE 4. Illustrating the variations in the geometry of the vocal folds over one cycle at intervals of 1/6 of a period according to the model of Zhao *et al.* (2002).

5. Voiced speech

5.1. *The vocal folds and glottis*

Voiced speech is produced by oscillations of the vocal folds induced by the application of a nominally steady 'subglottal' pressure from the lungs caused by respiratory musculature and passive elastic forces. Periodic vortex shedding from the 'tips' of the folds and feedback of pressure fluctuations produced by the convecting vorticity, drive the folds against elastic restoring forces into self-sustaining oscillations at frequencies f_o that rarely exceed 400 Hz for adult speakers (Flanagan 1972; Stevens 1998). The glottis is therefore acoustically compact and the principal acoustic modes excited in the vocal tract are in the form of plane progressive waves. Indeed, because the typical glottis flow velocity v approaches 20–40 m s^{-1}, the corresponding Strouhal number $f_o h/v$ ($\ll 1$) is much too small to permit the interaction with acoustic cross modes by mechanisms such as that mentioned by Boij & Nilsson (2003).

Figure 4 (adapted from Zhao *et al.* 2002) presents an idealized representation of the motion during a complete cycle at intervals of one sixth of a period ($1/f_o$). In the simplest approximation the shape of the glottis in sections normal to the axis of the vocal tract (the 'duct' axis) is a rectangle of fixed span ℓ_3 and continuously variable width $\Delta(x_1, t)$ (in the x_2 direction of figure 3).

Voicing is often initiated with the glottis tightly closed and subject to a subglottal over-pressure of about 10 cm of water ($\sim$1 kPa) – muscular adjustment ensuring

that this pressure is just sufficient to blow the folds apart. We shall model this theoretically in an attempt to expose the roles of the different source mechanisms by assuming that the motion starts with the arrival of a step pressure rise from the lungs which, combined with the muscular adjustment, causes the folds to begin to separate. Differences between different starting mechanisms affect only the shape of the initial acoustic transients, which usually decay during a small fraction of the vibration period.

When the step wave arrives (from the left in figure 4 and from $x_1 < 0$ in figure 3) the folds progressively separate and the glottis opens, initially forming a converging channel as indicated in figure 4(*b*). The subsequent depictions figures 4(*c*)–4(*f*) of the folds illustrate how separation is accompanied by a 'rocking' motion attributable to structural waves moving over the surfaces ('epithelia') of the folds (Stevens 1998). A constant over-pressure applied by the lungs causes the sequence of configurations in figure 4 to repeat periodically – except that we have shown the 'rest state' (figure 4*a*) to be one in which there is a small but finite glottal width $\Delta(x_1, t)$, in order to conform with the numerical investigation discussed in § 6. The actual variation of $\Delta(x_1, t)$ is determined by the simultaneous solution of equations of motion for the fluid and for the elastic vocal folds. Zhao *et al.* (2002) circumvented the extra complications presented by this combined system – thereby focusing attention on the fluid mechanics of sound generation – by introducing the following empirical model of the continuously variable glottal width during each cycle:

$$\Delta(x_1, t) = \tfrac{1}{2}(D_0 + D_{min} + (D_0 - D_{min})\tanh(\hat{s})) + D_{max}[1 - \tanh(\hat{s})] \times ((\hat{x} + \hat{c})\beta_1(T) - (\hat{x} - \hat{c})\beta_2(T)), \tag{5.1}$$

where $T = f_o t - [f_o t]$ is the fractional part of $f_o t$, the coordinate origin is taken on the main axis of symmetry at the centre of the glottis in its rest state,

$$\hat{s} = \hat{b}\left(|\hat{x}| - \frac{1}{|\hat{x}|}\right), \quad \hat{x} = \frac{x_1}{D_{max}}, \quad \hat{b} = 1.4, \quad \hat{c} = 0.42, \tag{5.2}$$

and

$$\beta_1(T) = \begin{cases} 0, & T \leqslant \frac{1}{9} \\ 0.244\left\{1 - \cos\left[\frac{9}{4}\pi\left(T - \frac{1}{9}\right)\right]\right\}, & \frac{1}{9} < T \leqslant \frac{5}{9}, \\ 0.488, & \frac{5}{9} < T \leqslant \frac{6}{9}, \\ 0.244\left\{1 + \cos\left[3\pi\left(T - \frac{6}{9}\right)\right]\right\}, & \frac{6}{9} < T < 1, \end{cases} \tag{5.3a}$$

$$\beta_2(T) = \beta_1\left(T + \tfrac{1}{9}\right). \tag{5.3b}$$

This model was used by Zhao *et al.* (2002) to investigate numerically voiced speech produced in a circular cylindrical vocal tract of diameter D_0 with an axisymmetric glottis. The minimum and maximum diameters of the glottis were respectively D_{min}, D_{max}, and characterize the respective situations in figures 4(*a*) and 4(*d*). We shall also use the empirical representation (5.1)–(5.3), but adapt it to the rectangular geometry discussed in § 4 by taking $D_0 = 2h$, with the more realistic rectangular glottis of span ℓ_3 and width $\Delta(x_1, t)$, with minimum and maximum widths equal to D_{min}, D_{max} respectively.

5.2. *Voice production as a scattering problem*

Let the incident over-pressure from the lungs consist of a step rise in pressure of amplitude p_I impinging on the glottis at $t = 0$. Then the corresponding incident total

enthalpy wave B_I can be written

$$B_I \equiv B_I\left(t-\frac{x_1}{c_o}\right) = \frac{p_I}{\rho_o}H\left(t-\frac{x_1}{c_o}\right). \tag{5.4}$$

Put $B = B_I + B_s$, where B_s is the field scattered at the glottis which has outgoing wave behaviour at large distances from the glottis. When the argument leading to (1.7) involving Green's theorem and the radiation condition is applied in the present case (with proper account taken of the contribution from the incident wave), we find

$$\begin{aligned} B_s(\boldsymbol{x},t) = &-\int(\boldsymbol{\omega}\wedge\boldsymbol{v})_j(\boldsymbol{y},\tau)\frac{\partial G}{\partial y_j}(\boldsymbol{x},\boldsymbol{y},t,\tau)\,\mathrm{d}^3\boldsymbol{y}\,\mathrm{d}\tau \\ &+\nu\oint_{S(\boldsymbol{y},\tau)}\boldsymbol{\omega}(\boldsymbol{y},\tau)\wedge\frac{\partial G}{\partial \boldsymbol{y}}(\boldsymbol{x},\boldsymbol{y},t,\tau)\cdot\mathrm{d}\boldsymbol{S}(\boldsymbol{y})\,\mathrm{d}\tau \\ &+\oint_{S(\boldsymbol{y},\tau)}G(\boldsymbol{x},\boldsymbol{y},t,\tau)\left(\frac{\partial v_j}{\partial\tau}+\frac{\partial B_I}{\partial y_j}\right)(\boldsymbol{y},\tau)\,\mathrm{d}S_j(\boldsymbol{y})\,\mathrm{d}\tau. \end{aligned} \tag{5.5}$$

In the final integral $\partial\boldsymbol{v}/\partial\tau+\partial B_I/\partial\boldsymbol{y}\equiv\partial\boldsymbol{v}_s/\partial\tau$, where $\boldsymbol{v}_s$ is the scattered component of velocity, and the term $\partial B_I/\partial\boldsymbol{y}$ represents the 'passive' scattering of the incident wave by the glottis geometry. To determine its contribution note from the definition (2.2) that the condition $\partial Y_1/\partial y_n \equiv \partial\{y_1-\varphi_1^*(\boldsymbol{y},\tau)\}/\partial y_n = 0$ on the instantaneous surface $\mathrm{S}(\boldsymbol{y},\tau)$ of the glottal folds implies that

$$\frac{\partial B_I}{\partial y_n} = -\frac{p_I}{\rho_o c_o}\delta\left(\tau-\frac{y_1}{c_o}\right)\frac{\partial\varphi_1^*}{\partial y_n} \approx -\frac{p_I}{\rho_o c_o}\delta(\tau)\frac{\partial\varphi_1^*}{\partial y_n}, \tag{5.6}$$

provided that it is permissible to neglect variations in the retarded time y_1/c_o within the glottal region.

Then

$$\begin{aligned} \oint_{S(\boldsymbol{y},\tau)}G\frac{\partial B_I}{\partial y_j}(\boldsymbol{y},\tau)\,\mathrm{d}S_j(\boldsymbol{y})\,\mathrm{d}\tau &\approx -\frac{p_I}{\rho_o c_o}\oint_{S(\boldsymbol{y},\tau)}G\delta(\tau)\nabla\varphi_1^*\cdot\mathrm{d}\boldsymbol{S}\,\mathrm{d}\tau \\ \equiv -\frac{p_I}{\rho_o c_o}\oint_{S(\boldsymbol{y},\tau)}G\frac{\partial}{\partial\tau}(H(\tau)\nabla\varphi_1^*)\cdot\mathrm{d}\boldsymbol{S}\,\mathrm{d}\tau &- \frac{p_I}{\rho_o c_o}\oint_{S(\boldsymbol{y},\tau)}GH(\tau)\frac{\partial}{\partial\tau}(\nabla Y_1)\cdot\mathrm{d}\boldsymbol{S}\,\mathrm{d}\tau \end{aligned} \tag{5.7}$$

where $G\equiv G(\boldsymbol{x},\boldsymbol{y},t,\tau)$. Because $\nabla Y_1\cdot\mathrm{d}\boldsymbol{S}\equiv 0$ on S, integration by parts reveals that the final integral in (5.7) is a second-order quantity, involving the small normal component of velocity on the vocal folds structure, and may therefore be discarded.

By recalling from (4.5) and the definition (2.2) that

$$\varphi_1^*(\boldsymbol{y},\tau)\sim\mp\frac{\ell(\tau)}{2}\quad\text{as}\quad y_1\to\pm\infty, \tag{5.8}$$

where $\nabla\varphi_1^*(\boldsymbol{y},\tau)$ decays exponentially fast as $|y_1|\to\infty$ in the vocal tract, it follows that

$$\begin{aligned} \oint_{S(\boldsymbol{y},\tau)}Y_1\frac{\partial}{\partial\tau}(H(\tau)\nabla\varphi_1^*)\cdot\mathrm{d}\boldsymbol{S}(\boldsymbol{y}) &= -\int\mathrm{div}\left(Y_1\frac{\partial}{\partial\tau}(H(\tau)\nabla\varphi_1^*)\right)\mathrm{d}^3\boldsymbol{y} \\ &= -\int\mathrm{div}\left(\nabla Y_1\frac{\partial}{\partial\tau}(H(\tau)\varphi_1^*)\right)\mathrm{d}^3\boldsymbol{y} = \mathscr{A}\frac{\partial}{\partial\tau}(H(\tau)\ell(\tau)), \end{aligned} \tag{5.9}$$

and therefore that the first term on the second line of (5.7) yields

$$\oint_{S(\boldsymbol{y},\tau)} G\frac{\partial B_I}{\partial y_j}(\boldsymbol{y},\tau)\,\mathrm{d}S_j(\boldsymbol{y})\,\mathrm{d}\tau \approx -\frac{p_I}{\rho_o}\frac{\mathrm{sgn}(x_1)}{\ell([t])}\int_{-\infty}^{[t]}\frac{\partial}{\partial\tau}(H(\tau)\ell(\tau))\exp\left(-\int_\tau^{[t]}\frac{2c_o\,\mathrm{d}\xi}{\ell(\xi)}\right)\mathrm{d}\tau. \tag{5.10}$$

Using this result, and putting $B = B_I + B_s$ into (5.5), we may now express the solution in the form

$$\begin{aligned} B(\boldsymbol{x},t) = {} & \frac{p_I}{\rho_o}\left\{H\left(t-\frac{x_1}{c_o}\right) - \frac{\mathrm{sgn}(x_1)}{\ell([t])}\int_{-\infty}^{[t]}\frac{\partial}{\partial\tau}(H(\tau)\ell(\tau))\exp\left(-\int_\tau^{[t]}\frac{2c_o\,\mathrm{d}\xi}{\ell(\xi)}\right)\mathrm{d}\tau\right\} \\ & - \int(\boldsymbol{\omega}\wedge\boldsymbol{v})_j(\boldsymbol{y},\tau)\frac{\partial G}{\partial y_j}(\boldsymbol{x},\boldsymbol{y},t,\tau)\,\mathrm{d}^3\boldsymbol{y}\,\mathrm{d}\tau + \nu\oint_{\boldsymbol{S}(\boldsymbol{y},\tau)}\boldsymbol{\omega}(\boldsymbol{y},\tau)\wedge\frac{\partial G}{\partial\boldsymbol{y}}(\boldsymbol{x},\boldsymbol{y},t,\tau)\cdot\mathrm{d}\boldsymbol{S}(\boldsymbol{y})\,\mathrm{d}\tau \\ & + \oint_{S(\boldsymbol{y},\tau)} G(\boldsymbol{x},\boldsymbol{y},t,\tau)\frac{\partial v_j}{\partial\tau}(\boldsymbol{y},\tau)\,\mathrm{d}\boldsymbol{S}_j(\boldsymbol{y})\,\mathrm{d}\tau,\ [t] = t - \frac{|x_1|}{c_o}. \end{aligned} \tag{5.11}$$

The term

$$-\frac{p_I}{\rho_o}\frac{\mathrm{sgn}(x_1)}{\ell([t])}\int_{-\infty}^{[t]}\frac{\partial}{\partial\tau}(H(\tau)\ell(\tau))\exp\left(-\int_\tau^{[t]}\frac{2c_o\,\mathrm{d}\xi}{\ell(\xi)}\right)\mathrm{d}\tau$$

represents a transient response to the incident step rise in pressure. It decays rapidly to zero after a retarded time $\sim\ell/c_o$, where ℓ is the characteristic value of the glottis end-correction following its impulsive opening. At later times – ignoring for the moment the influence of the remaining integrated terms in (5.11) – the incident step pressure wave can be said to be fully transmitted through the glottis without attenuation. In the region $x_1 < 0$ this term represents a transient reflected pressure pulse of width $\sim\ell$ radiated back to the lungs.

5.3. *Vortex sound*

These transient motions dominate the scattered sound immediately after the arrival of the step wave. The remaining integrals in (5.11) involving vorticity and surface accelerations are initially small because, for example, vorticity must first be convected into the flow after shedding from the folds by the very low-Mach-number glottal mean flow. At later times, the flow just downstream of the glottis forms a jet of nominally rectangular cross-section of span ℓ_3 whose width is modulated by the continuously varying width of the glottis. The jet is unstable and this ordered picture is not maintained further downstream, where the flow becomes locally dominated by turbulence and the formation of large vortical structures, but this actually occurs at a sufficient distance from the glottis that the efficiency of sound generation during breakdown is negligible. The strength of the vortex sound B_ω, say, is governed by the volume integral on the second line of (5.11), which can be evaluated in the forms

$$\begin{aligned} B_\omega = {} & -\int(\boldsymbol{\omega}\wedge\boldsymbol{v})_j(\boldsymbol{y},\tau)\frac{\partial G}{\partial y_j}(\boldsymbol{x},\boldsymbol{y},t,\tau)\,\mathrm{d}^3\boldsymbol{y}\,\mathrm{d}\tau \\ & \approx -\frac{c_o\mathrm{sgn}(x_1)}{\mathscr{A}\ell([t])}\int_{-\infty}^{[t]}\exp\left(-\int_\tau^{[t]}\frac{2c_o d\xi}{\ell(\xi)}\right)\mathrm{d}\tau\int\left(\frac{\partial Y_1}{\partial\boldsymbol{y}}\cdot\boldsymbol{\omega}\wedge\boldsymbol{v}\right)(\boldsymbol{y},\tau)\,\mathrm{d}^3\boldsymbol{y} \quad (5.12a) \\ & \approx -\frac{\mathrm{sgn}(x_1)}{2\mathscr{A}}\left[\int\frac{\partial Y_1}{\partial\boldsymbol{y}}\cdot\boldsymbol{\omega}\wedge\boldsymbol{v}\,\mathrm{d}^3\boldsymbol{y}\right]_{t-|x_1|/c_o}, \quad (5.12b) \end{aligned}$$

where the approximation (5.12*b*) is applicable provided the characteristic time $\sim 1/f_o$ of vortex formation satisfies $f_o\ell/c_o \ll 1$ (i.e. the glottis is acoustically compact).

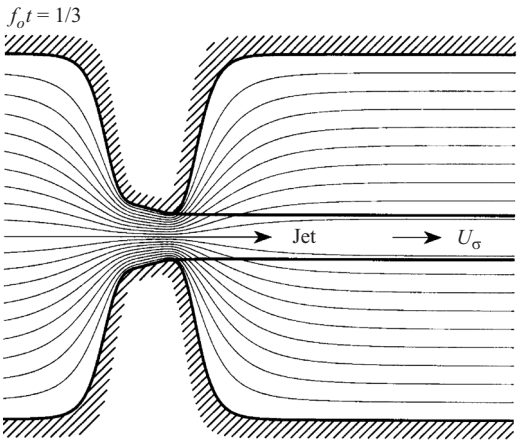

FIGURE 5. Emerging jet modelled as a quasi-static free streamline flow with asymptotic jet speed U_σ at stage (c) of figure 4. The majority of the 'streamlines' of the Green's function velocity potential $Y_1(\boldsymbol{x}, t)$ cut the jet boundary typically within a distance downstream of the glottis of the order of the glottal width.

Figure 5 illustrates the streamline structure of the 'flow' defined by the velocity potential Y_1 of figure 4(c). Sound is generated strongly (i.e. with dipole strength as opposed to the much quieter quadrupole strength of free turbulence sources) in regions where the streamline pattern varies rapidly, on scales comparable to those of the vortex field. This is evidently the region just downstream of the glottis within a distance equal roughly to the glottal width – further downstream, the streamlines become uniformly spaced and parallel and ∇Y_1 varies very slowly. The integration in (5.12) can then be evaluated by holding $\partial Y_1/\partial \boldsymbol{y}$ constant over the region occupied by a coherent eddy, in which case $\int \boldsymbol{\omega} \wedge \boldsymbol{v}\, \mathrm{d}^3\boldsymbol{y} = 0$ when the eddy is compact: under these circumstances the sound generated by the eddy is of quadrupole type.

Figure 5 also illustrates the consequence of the hypothesis that the Reynolds number based on the glottis length and flow velocity is large, so that vorticity shed from the glottis is initially confined to 'free streamlines' at the edges of the jet. From what has been said above, it is only necessary for this approximation to be adequate within a distance of about one glottal width downstream, where the Green's function streamlines of the potential Y_1 cut across the jet boundary. On this boundary, the flow speed is constant and equal to U_σ, say, the asymptotic jet velocity predicted by free streamline theory (Birkhoff & Zarantonello 1957; Gurevich 1965). Thus, for example, along the upper free streamline of figure 5, the vorticity $\boldsymbol{\omega} = U_\sigma \delta(s_\perp)\boldsymbol{k}$ where $s_\perp$ is the distance measured in the direction of the outward normal from the free streamline and $\boldsymbol{k}$ is a unit vector out of the plane of the paper; the vorticity convection velocity $\boldsymbol{v} = U_\sigma \mathbf{t}/2$, where $\boldsymbol{t}$ is a unit vector tangential to the free streamline flow. Hence, because $\boldsymbol{k} \wedge \boldsymbol{t}$ is the unit normal directed outwards from the jet, the contributions from both edges of the jet can be combined to yield

$$\int \left(\frac{\partial Y_1}{\partial \boldsymbol{y}} \cdot \boldsymbol{\omega} \wedge \boldsymbol{v} \right) (\boldsymbol{y}, \tau)\, \mathrm{d}^3\boldsymbol{y} = \ell_3 U_\sigma^2(\tau) \int_0^\infty \left(\frac{\partial Y_1}{\partial s_\perp} \right)_{s_\perp = 0} \mathrm{d}s,$$

where s is the distance measured along a free streamline from the glottis. Now $2\ell_3 \int_0^\infty (\partial Y_1/\partial s_\perp)_{s_\perp=0}\, \mathrm{d}s = \mathscr{A}$, provided the asymptotic jet width is small compared to the width $2h$ of the vocal tract. Therefore the vortex sound formulae (5.12a, b),

respectively, become

$$B_\omega \approx -\frac{c_o \mathrm{sgn}(x_1)}{2\ell([t])} \int_{-\infty}^{[t]} U_\sigma^2(\tau) \exp\left(-\int_\tau^{[t]} \frac{2c_o\,\mathrm{d}\xi}{\ell(\xi)}\right) d\tau \tag{5.13a}$$

$$\approx -\frac{\mathrm{sgn}(x_1)}{4} U_\sigma^2(t - |x_1|/c_o). \tag{5.13b}$$

5.4. *The monopole sound*

Cyclic motion of the vocal folds is accompanied by small periodic changes in their volume and the consequent production of a monopole component of sound that radiates as equal waveforms in both directions away from the glottis. It will be denoted by B_m, and is the principal contribution from the last integral in (5.11) which, after discarding a smaller surface-generated dipole, yields

$$B_m \approx \frac{c_o}{2\mathscr{A}} \left[\oint_S \boldsymbol{v}\cdot \mathrm{d}\boldsymbol{S}\right]_{t-|x_1|/c_o} = -\frac{c_o \ell_3}{2\mathscr{A}} \frac{\partial}{\partial t} \int_{-\infty}^{\infty} \Delta\left(y_1, t - \frac{|x_1|}{c_o}\right) \mathrm{d}y_1. \tag{5.14}$$

5.5. *Solution of the scattering problem*

The remaining viscous term in (5.9) is associated predominantly with frictional drag in the glottis. It becomes significant as the local Reynolds number becomes small, when $\Delta \to 0$. We shall, however, ignore its contribution to the acoustic field because the end-correction $\ell \to \infty$ as the glottis closes, causing the overall radiation to drop to zero. Hence, collecting together the principal contributors to the solution (5.11), and putting $B(\boldsymbol{x}, t) = p(x_1, t)/\rho_o$ in the acoustic region, we can write

$$p(x_1, t) = p_I \left\{ H\left(t - \frac{x_1}{c_o}\right) - \frac{\mathrm{sgn}(x_1)}{\ell([t])} \int_{-\infty}^{[t]} \frac{\partial}{\partial \tau}(H(\tau)\ell(\tau)) \exp\left(-\int_\tau^{[t]} \frac{2c_o\,d\xi}{\ell(\xi)}\right) \mathrm{d}\tau \right\}$$

$$- \frac{\rho_o c_o \mathrm{sgn}(x_1)}{2\ell([t])} \int_{-\infty}^{[t]} U_\sigma^2(\tau) \exp\left(-\int_\tau^{[t]} \frac{2c_o\,\mathrm{d}\xi}{\ell(\xi)}\right) \mathrm{d}\tau - \frac{\rho_o c_o \ell_3}{2\mathscr{A}} \frac{\partial}{\partial t} \int_{-\infty}^{\infty} \Delta(y_1, [t])\,\mathrm{d}y_1,$$

$$\text{where} \quad [t] = t - \frac{|x_1|}{c_o}. \tag{5.15}$$

The vortex sound term on the second line of this formula is actually approximated well by (5.13*b*) at all times when its contribution is significant.

6. Numerical prediction of voiced sounds

6.1. *Computation of the sound*

The final monopole component of (5.15) is readily evaluated without further analysis in terms of the vocal fold shape functions (5.1)–(5.3). To compute the remaining terms in (5.15) we put

$$p'(x_1, t) = p_I \left\{ H\left(t - \frac{x_1}{c_o}\right) - \frac{\mathrm{sgn}(x_1)}{\ell([t])} \int_{-\infty}^{[t]} \frac{\partial}{\partial \tau}\Big(H(\tau)\ell(\tau)\Big) \exp\left(-\int_\tau^{[t]} \frac{2c_o\,\mathrm{d}\xi}{\ell(\xi)}\right) \mathrm{d}\tau \right\}$$

$$- \frac{\rho_o c_o \mathrm{sgn}(x_1)}{2\ell([t])} \int_{-\infty}^{[t]} U_\sigma^2(\tau) \exp\left(-\int_\tau^{[t]} \frac{2c_o\,\mathrm{d}\xi}{\ell(\xi)}\right) \mathrm{d}\tau. \tag{6.1}$$

For $x_1 > 0$, the acoustic particle velocity of this outgoing wave is equal to $p'(x_1, t)/\rho_o c_o$. Let

$$U(t) = \lim_{x_1 \to +0} \frac{p'(x_1, t)}{\rho_o c_o} \tag{6.2}$$

be the limiting value of this velocity just to the right of the glottis in figure 3 (i.e. $x_1 \sim +0$ so that $[t] \to t$). Then by differentiating the corresponding limit of (6.1) we find

$$\frac{\mathrm{d}(\ell U)}{\mathrm{d}t} + 2c_o U + \tfrac{1}{2}U_\sigma^2 = \frac{2p_I}{\rho_o} H(t). \tag{6.3}$$

This is reduced to an ordinary differential equation for $U(t)$ by defining $\Delta_m(t)$ to be the minimum width of the glottis at time t. Then, because the flow in the neighbourhood of the glottis can be considered to be incompressible,

$$U_\sigma \approx \frac{\mathscr{A}U}{\ell_3 \sigma \Delta_m} \equiv \frac{2hU}{\sigma \Delta_m}, \tag{6.4}$$

where σ is the contraction ratio of the jet, defined such that σU_σ is the jet velocity at the position of the glottal minimum, from where the free streamlines may be assumed to emerge. Therefore, the near-field limit U of the acoustic particle velocity satisfies

$$\frac{\mathrm{d}(\ell U)}{\mathrm{d}t} + 2c_o U + 2\left(\frac{h}{\sigma \Delta_m(t)}\right)^2 U^2 = \frac{2p_I}{\rho_o} H(t). \tag{6.5}$$

The causal solution of this equation and the relation (6.4) determine the jet velocity U_σ for substitution into the acoustic pressure formula (5.15). However, it is unnecessary to do this because knowledge of the near-field value of the acoustic particle velocity $U(t)$ immediately supplies the following expressions for the overall acoustic pressure

$$p(x_1, t) = \rho_o c_o U\left(t - \frac{x_1}{c_o}\right) - \frac{\rho_o c_o \ell_3}{2\mathscr{A}} \frac{\partial}{\partial t} \int_{-\infty}^{\infty} \Delta\left(y_1, t - \frac{x_1}{c_o}\right) \mathrm{d}y_1, \quad x_1 \to +\infty \tag{6.6a}$$

$$= p_I \left[H\left(t - \frac{x_1}{c_o}\right) + H\left(t + \frac{x_1}{c_o}\right)\right] - \rho_o c_o U\left(t + \frac{x_1}{c_o}\right)$$
$$- \frac{\rho_o c_o \ell_3}{2\mathscr{A}} \frac{\partial}{\partial t} \int_{-\infty}^{\infty} \Delta\left(y_1, t + \frac{x_1}{c_o}\right) \mathrm{d}y_1, \quad x_1 \to -\infty. \tag{6.6b}$$

6.2. *The electrical analogue*

Our deduction of (6.5) from the nonlinear equations of motion supports the lumped-parameter approximation originally used to study voicing (Fant 1960; Flanagan 1972). This is based on an analogy that models the vocal system as an electrical transmission line. The glottis is interpreted as a 'monopole' source of voiced sound whose strength $Q \equiv U\mathscr{A}$ is the unsteady glottal volume flux, in terms of which (6.5) becomes

$$\frac{d(\ell Q)}{\mathrm{d}t} + 2c_o Q + \frac{2}{\mathscr{A}}\left(\frac{h}{\sigma \Delta_m(t)}\right)^2 Q^2 = \frac{2p_I}{\rho_o} \mathscr{A} H(t). \tag{6.7}$$

The electrical analogy furnishes (Fant 1960)

$$\rho_o \ell \frac{\mathrm{d}Q}{\mathrm{d}t} + K Q^2 = \Delta p \mathscr{A}, \tag{6.8}$$

in which an inductive load (first term on the left-hand side) and a nonlinear resistance with 'loss factor' K are balanced against the pressure force $\Delta p \mathscr{A}$ across the glottis. In detailed modelling with this equation, the value of the pressure load Δp should

be adjusted to account properly for the acoustic admittances of the vocal tract on each side of the glottis (Lighthill 1978). This is usually done indirectly by iteration (Ananthapadmanabha & Fant 1982). In our case of (6.7), of course, no attempt has been made to take account of vocal tract acoustics, in that we have assumed radiation from the glottis to occur as in an infinite uniform duct, without reflections and other interactions occurring at remote points in the vocal tract.

The conventional 'monopole' interpretation of the overall source of voiced speech is obviously incorrect, but it does provide a convenient working model that is often useful. Its existence has frequently been challenged (Teager & Teager 1983; McGowan 1988; Hirschberg 1992; Hofmans 1998; Barney, Shadle & Davies 1999; Mongeau *et al.* 1997; Shadle *et al.* 1999). McGowan (1988) argued that vorticity is produced at the glottis and that a significant part of the generated sound must therefore be of dipole origin, although he did not quantify his argument. The predominantly dipole character of voiced sounds was established by the numerical work of Zhao *et al.* (2002), who showed that the principal source is the fluctuating surface pressures on the vocal folds.

6.3. *Role of the unsteady end-correction*

The end-correction $\ell(t)$ is evaluated for any configuration of the glottis using the definition (4.6). To do this, it is generally necessary to determine the Kirchhoff vector $Y_1(\boldsymbol{x}, t)$ by numerical integration of $\nabla^2 Y_1 = 0$ subject to the conditions $\partial Y_1/\partial x_1 \to 1$ as $x_1 \to \pm\infty$ and $\partial Y_1/\partial x_n = 0$ on the walls of the vocal tract and glottis (in the present case, the problem is two-dimensional and it is simpler to solve Laplace's equation for the corresponding stream function, which assumes constant values on the walls). When voicing occurs at a fixed frequency f_o, the calculation must be performed for a range of times over a typical period of duration $1/f_o$.

A preliminary picture of the expected dependence of ℓ on time is easily obtained for the case depicted in figure 6 where a 'glottis' of width $\Delta(t)$ is formed by the gap between rudimentary vocal folds of infinitesimal thickness, for which

$$\frac{\ell(t)}{h} = \frac{4}{\pi} \ln\left\{\frac{1}{2}\left[\tan\left(\frac{\pi\Delta(t)}{8h}\right) + \cot\left(\frac{\pi\Delta(t)}{8h}\right)\right]\right\}. \tag{6.9}$$

By way of illustration we take

$$\Delta(t) = \frac{1}{2}(D_{max} + D_{min}) - \frac{1}{2}(D_{max} - D_{min})\cos(2\pi f_o t). \tag{6.10}$$

The curves in figure 6(*b*) show the variation of $\ell(t)/h$ over a complete cycle for the two cases in which minimum glottal widths are $D_{min} = 0.02h$, $0.002h$ and when $D_{max}/h = 0.4$. In both cases ℓ assumes its minimal values when Δ is large, and rises to logarithmically large peak values at $\Delta = D_{min}$. The maxima attained for a more realistic glottis model, such as that defined by (5.1)–(5.3) (Zhao *et al.* 2002), can be expected to be much larger, because the section of the infinite range of integration in (4.6) within which $\partial Y_1/\partial x_1$ is very large now extends over the finite axial length of the glottis.

Figure 7 shows the corresponding variation of the end-correction when the vocal folds are defined by our two-dimensional adaptation of the Zhao *et al.* (2002) model (5.1)–(5.3) and

$$D_0 \equiv 2h = 20\,\text{mm}, \quad D_{min} = 0.1\,\text{mm}, \quad D_{max} = 4\,\text{mm}. \tag{6.11}$$

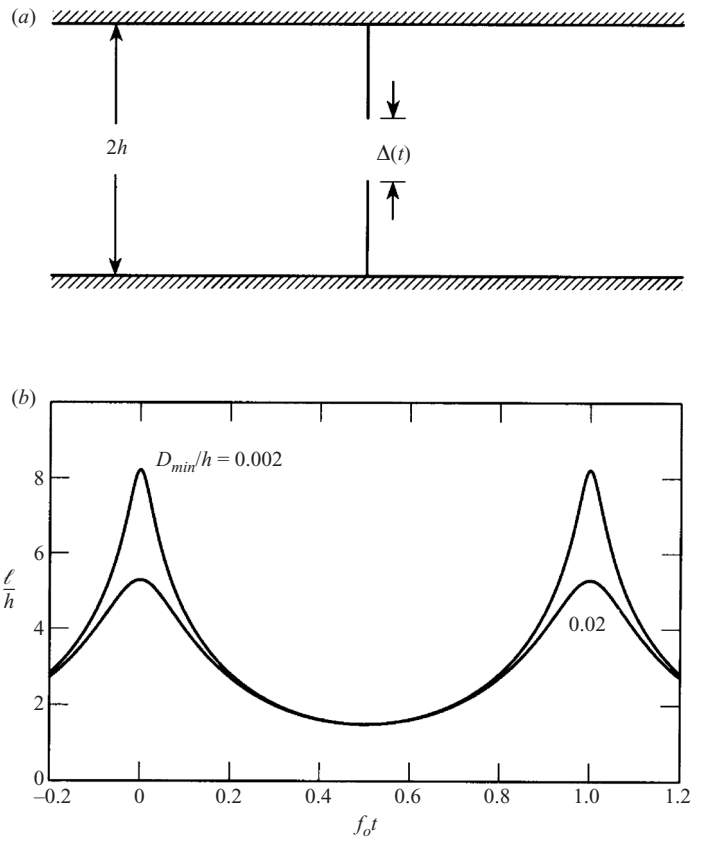

FIGURE 6. Variation of the end-correction $\ell(t)$ for the rudimentary two-dimensional glottis formed by the slit between vocal folds of infinitesimal thickness defined by (6.9), for the two cases where $D_{max}/h = 0.4$, $D_{min}/h = 0.02$ and 0.002.

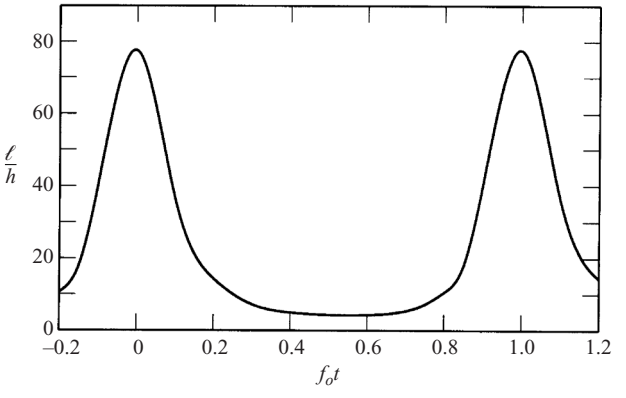

FIGURE 7. Variation of the end correction $\ell(t)$ during periodic motion of the glottis for the Zhao *et al.* (2002*b*) model defined by equations (5.1)–(5.3) when $D_0 \equiv 2h = 20\,\text{mm}$, $D_{min} = 0.1\,\text{mm}$, $D_{max} = 4\,\text{mm}$.

The general dependence of ℓ on the glottal width is the same as in figure 6 for the slit glottis, but the peak values attained when Δ tends towards closure are much larger.

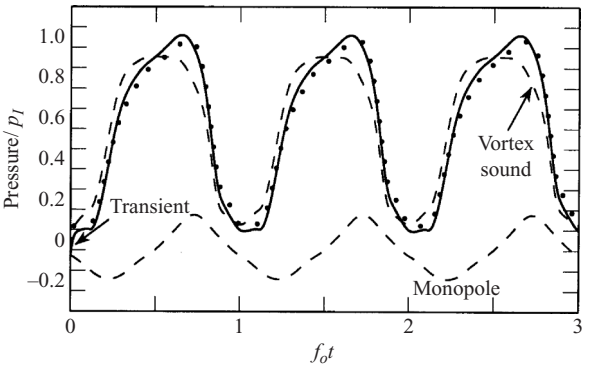

FIGURE 8. The first two cycles of the pressure (6.6*a*) (——) radiated from the glottis towards the mouth ($x_1 > 0$) for conditions (6.11) when $f_0 = 125\,\mathrm{Hz}$ and $p_I = 8\,\mathrm{cm}$ of water. Also shown (- - - -) are the separate contributions from the vortex sound superimposed on the mean transmitted pressure p_I and the monopole sound (5.14). The dotted curve (···) is the quasi-static approximation (6.12).

The first three cycles of the pressure wave radiated towards the mouth ($x_1 > 0$) for this mode of oscillation of the vocal folds are determined by (6.6*a*) and illustrated in figure 8 for an incident step pressure rise of $p_I = 8\,\mathrm{cm}$ of water ($\sim 0.8\,\mathrm{kPa}$; it being also assumed that $c_o = 340\,\mathrm{m\,s^{-1}}$, $\rho_o = 1.23\,\mathrm{kg\,m^{-3}}$). The frequency $f_o = 125\,\mathrm{Hz}$, which is typical of an adult male. The figure shows the overall predicted waveform of the sound and the separate contributions from the vortex sound term $\rho_o c_o U$ of (6.6*a*) (superimposed on the mean transmitted pressure of amplitude p_I) and the monopole (5.14). Equation (6.5) has been integrated using a fourth-order Runge–Kutta routine, and the simplest approximation has been adopted in which the jet contraction ratio $\sigma = 1$, although it should be realized that the detailed behaviour of σ depends in a complicated way on Reynolds number and surface motion during the opening and closing phases of the glottal motion (Krane & Wei 2006; Park & Mongeau 2007).

The rapid transient build-up of the transmitted sound to its periodic form occupies a small fraction of a cycle, as indicated in the figure. The shape of this transient is controlled by the first, differentiated term on the left-hand side of (6.5). When this is discarded, the solution of the resulting quadratic equation yields the quasi-static approximation

$$U(t) = \frac{c_o}{2}\frac{\sigma \Delta_{\mathrm{m}}(t)}{h}\left(\sqrt{\left(\frac{\sigma \Delta_m(t)}{h}\right)^2 + \frac{4p_I}{\rho_o c_o^2}} - \frac{\sigma \Delta_m(t)}{h}\right), \quad t > 0. \tag{6.12}$$

The prediction of the sound using this formula in (6.6*a*) is plotted as the dotted curve in figure 8. Evidently the neglect of the 'inductive' term in (6.5) results in a prediction that lacks an initial transient but is otherwise a very close approximation to the full predicted acoustic pressure. For practical purposes, therefore, it appears that the quasi-static representation of the sound is quite adequate, a conclusion that is consistent with experiments reported by Zhang, Mongeau & Frankel (2002) and Park & Mongeau (2007).

Thus, the dominant influence of the variable end-correction $\ell(t)$ is actually confined to the initial phases of sound generation. At later times, the transmitted pressure remains positive and always exceeds about $0.1 p_I$. This is because for a rectangular glottis of elongated span $\ell_3 \sim O(h)$, the periodic reduction of its width to a minimum

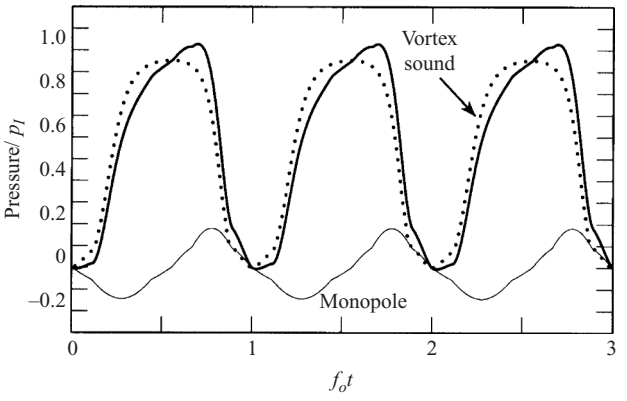

FIGURE 9. The quasi-static approximation to the pressure (6.6*a*) (———) radiated from the glottis towards the mouth ($x_1 > 0$) for conditions (6.13) when $f_0 = 125\,\mathrm{Hz}$ and $p_I = 8\,\mathrm{cm}$ of water. Also shown are the separate contributions from the vortex sound superimposed on the mean transmitted pressure p_I and the monopole sound (5.14).

value $D_{min} = 0.1\,\mathrm{mm}$ ($= 0.01h$) is not sufficient to impede the transmission of acoustic energy. This may be contrasted with the numerical results of Zhao *et al.* (2002) for a similarly profiled glottis of circular cross-section, where the radiated pressure consisted of a series of positive pulses whose amplitude effectively reduces to zero at retarded times at which the glottis diameter is a minimum.

The net contribution from the monopole sound produced by volumetric changes of the vocal folds alternates in sign as the folds expand and contract to modulate the glottal width and furnishes a small correction to the overall wave profile. It is clear from (6.6) that the amplitude of this source would be expected to increase with frequency, although it is actually believed that an increase in the frequency of oscillation of the folds is accompanied by other structural changes that tend to oppose a corresponding increase in volume fluctuations (Stevens 1998).

6.4. *The quasi-static approximation*

In voiced speech, the periodic motions of the vocal folds usually include intervals in which the glottis is closed, the exception being the special case of 'breathy' voicing (Fant 1960; Flanagan 1972). The influence of closure is easily included in the quasi-static approximation, whereas the corresponding change in the connectivity of the three-dimensional space forming the vocal tract would require special treatment of the full equation (6.5), involving a limiting process in which $\ell/h \to \infty$.

Thus, when conditions (6.11) for the two-dimensional Zhao *et al.* (2002) model (5.1)–(5.3) are replaced by

$$D_0 \equiv 2h = 20\,\mathrm{mm}, \quad D_{min} = 0\,\mathrm{mm}, \quad D_{max} = 4\,\mathrm{mm}, \tag{6.13}$$

the glottis is fully closed in the configuration in figure 4(*a*). Figure 9 illustrates the quasi-static approximation for the sound radiated towards the mouth when $f_0 = 125\,\mathrm{Hz}$ and $p_I = 8\,\mathrm{cm}$ of water. The dotted and thin line curves, respectively, show the separate contributions from the vortex sound superimposed on the mean transmitted pressure p_I and the vocal folds monopole. The waveform consists of a succession of acoustic pulses separated by instances of zero amplitude.

Figure 10 depicts a similar prediction for the more usual case in which the glottis (again defined by conditions (6.12) and the two-dimensional Zhao *et al.* (2002)

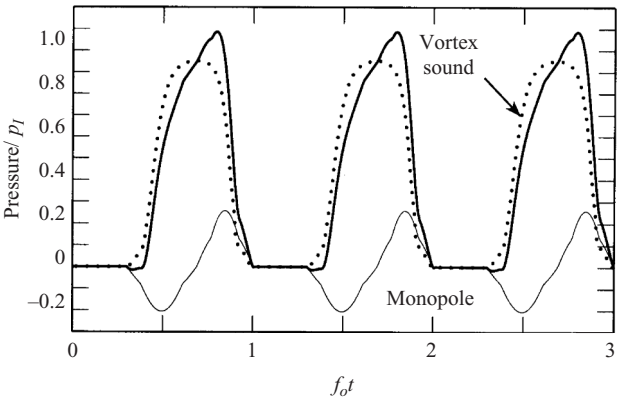

FIGURE 10. As for figure 9 with $f_0 = 125\,\text{Hz}$ and $p_I = 8\,\text{cm}$ of water, but in the case where the glottis remains closed during the first 30 % of each cycle, producing a succession of pressure pulses separated by short intervals of 'silence'.

model) is closed for a finite fraction of each cycle and varies as in figure 4 during the remainder of the cycle. It is assumed that $f_0 = 125\,\text{Hz}$ and $p_I = 8\,\text{cm}$ of water, but that the glottis is closed during the first 30 % of each cycle. Successive pressure pulses are now separated by short intervals of 'silence'. The maximum amplitude of the vortex sound is unchanged from that shown in figure 9 because the net variation in glottal area is the same; however, the contribution from the monopole is increased because the volumetric changes of the folds occur more rapidly.

7. Conclusion

The sound produced by aerodynamic sources near a compact body, or near a compact surface feature on a large boundary, is usually dominated by monopole and dipole components. The monopole is absent for rigid bodies or for deformable bodies of invariable volume. To make detailed predictions – as opposed to general order of magnitude estimates – it is necessary to have an intimate knowledge of the source flow. At low Mach numbers, it is usually permissible to ignore fluid compressibility when investigating this near-field motion, which can then be 'mapped' into the radiating sound by employing a suitable aeroacoustic Green's function. Alternatively, lengthy but nominally precise numerical treatments of the full equations of motion can be used to predict the whole flow simultaneously, although many problems are too complex even for the fastest of present day computers to make this practicable. Such approaches also tend to be expensive, rarely supply predictions in a timely manner, and frequently provide little of the insight required to formulate effective noise-control procedures.

The recognition that the most efficient sources of sound at low Mach numbers are generally associated with flow structures within compact regions of a larger flow has encouraged the development of the compact Green's function, and its extension in this paper to deal with compact bodies that can deform in an essentially arbitrary manner. Howe *et al.* (2006) have demonstrated how the application of this method to low-frequency sound generated by a high-speed train can provide rapid and accurate predictions in a case involving extensive non-compact source distributions, and where a numerical treatment would consume tens or hundreds of hours of CPU time.

Our discussion of voiced speech similarly permits a detailed interpretation to be made of the different source mechanisms. The principal source is a dipole produced by a nonlinear coupling of vorticity with the vocal folds; only vorticity within about one glottal width of the folds was shown to participate effectively in this interaction. The strength of the source is governed by the integral in equation (5.12*b*), which is actually proportional to the hydrodynamic drag on the folds (Howe 1998, 2003; Stevens 1998, p. 65; Biesheuvel & Hagmeijer 2006). This is in accord with the numerical conclusion of Zhao *et al.* (2002), who deduced the dominance of vocal fold surface forces by calculation of the sources contributing to the Ffowcs Williams – Hawkings (1969) representation of the sound. The subsequent unstable development of the vortex wake downstream of the glottis may, in practice, be responsible for 'noisy' interactions with vocal tract appendages, but has little or no influence on voiced sounds, although its quantification occupies a considerable fraction of computer time in a numerical treatment.

The discussion in § 6 of a spanwise-elongated rectangular glottis is arguably more realistic than the circular glottis considered by Zhao *et al.* (2002), but neither model is ideal. An orifice bears little relation to the actual geometry, and the rectangular glottis is acoustically too 'transparent'. However, although no detailed measurements of voice signals are available, the numerical predictions of Zhao *et al.* (2002) and our waveforms presented in figures 8 to 10 are mutually consistent and in general accord with typical voice signatures reported in the literature (e.g. Flanagan 1972; Stevens 1998). The conclusion that voiced sounds are probably approximated well by the quasi-static approximation (6.11) admits of the following generalization of the formula for the acoustic-dipole pressure for a glottis of arbitrary shape

$$p(x_1,t) = \frac{Q(t-x_1/c_0)}{(\mathscr{A}/\rho_o c_o)} = \left[\frac{\rho_o c_o^2}{2}\frac{\sigma\mathscr{A}_m(t)}{\mathscr{A}}\left(\sqrt{\left(\frac{\sigma\mathscr{A}_m(t)}{\mathscr{A}}\right)^2+\frac{4p_I(t)}{\rho_o c_o^2}}-\frac{\sigma\mathscr{A}_m(t)}{\mathscr{A}}\right)\right]_{t-x_1/c_o}, \quad (7.1)$$

where Q is the unsteady volume flux through the glottis (the 'monopole' source strength of Fant 1960), $p_I(t)$ is the subglottal over-pressure applied to the vocal folds and $\mathscr{A}_m(t)$ is the minimum glottal cross-section at time t. The ratio $\mathscr{A}/\rho_o c_o$ is the acoustic admittance of the vocal tract when modelled (as in this paper) as a uniform semi-infinite duct (Lighthill 1978). A formula very like (7.1) has been examined by Park & Mongeau (2007), who concluded from a series of measurements involving convergent and divergent glottis-shaped orifices that the approximation is applicable during about 70 % of a typical glottal cycle (a similar conclusion was drawn by Zhang *et al.* 2002). However, a fully self-consistent application of the general method of this paper to the vocal tract, with its complex system of formants, requires the derivation of Green's function in § 4 to be modified to take account of the radiation properties (the admittance) of the vocal tract on either side of the glottis. The acoustic particle velocity U would then satisfy a nonlinear, integro-differential equation (instead of (6.5)), and the quasi-static approximation that corresponds to (7.1) would need to be derived numerically.

This work was partially supported by grant NIDCD-004688 to Dr G. Berke of UCLA.

REFERENCES

Ananthapadmanabha, T. V. & Fant, G. 1982 Calculation of the true glottal flow and its components. *Speech Commun.* **1**, 167–184.

Baker, B. B. & Copson, E. T. 1969 *The Mathematical Theory of Huygen's Principle*, 2nd edn. Oxford University Press.

Barney, A., Shadle, C. H., & Davies, P. O. A. L. 1999 Fluid flow in a dynamic mechanical model of the vocal folds and tract. *J. Acoust. Soc. Am.* **105**, 444–455.

Batchelor, G. K. 1967 *An Introduction to Fluid Dynamics*. Cambridge University Press.

Beranek L. L. & Vér, I. L. (ed.) 1992 *Noise and Vibration Control Engineering*. John Wiley.

Biesheuvel, A. & Hagmeijer, R. 2006 On the force on a body moving in a fluid. *Fluid Dyn. Res.* **38**, 716–742.

Birkhoff, G. and Zarantonello, E. H. 1957 *Jets, Wakes and Cavities*. Academic.

Boij, S. & Nilsson, B. 2003 Reflection of sound at area expansions in a flow duct. *J. Sound Vib.* **260**, 477–498.

Crighton D. G. 1975*a* Basic principles of aerodynamic noise generation. *Prog. Aerospace Sci.* **16**, 31–96.

Crighton, D. G. 1975*b* Scattering and diffraction of sound by moving bodies. *J. Fluid Mech.* **72**, 209–227.

Crighton, D. G. & Leppington, F. G. 1971 On the scattering of aerodynamic noise. *J. Fluid Mech.* **46**, 577–597.

Crighton, D. G., Dowling, A. P., Ffowcs Williams, J. E., Heckl, M. & Leppington, F. G. 1992 *Modern Methods in Analytical Acoustics* Lecture Notes. Springer.

Curle, N. 1955 The influence of solid boundaries upon aerodynamic sound. *Proc. R. Soc. Lond.* A **231**, 505–514.

Duncan, C., Zhai, G. & Scherer, R. 2006 Modeling coupled aerodynamics and vocal fold dynamics using immersed boundary methods. *J. Acoust. Soc. Am.* **120**, 2859–2871.

Fant, G. 1960 *Acoustic Theory of Speech Production*. Mouton, The Hague.

Ffowcs Williams, J. E. & Hawkings, D. L. 1969 Sound generation by turbulence and surfaces in arbitrary motion. *Phil. Trans. Roy. Soc.* A **264**, 321–342.

Flanagan, J. L. 1972 *Speech Analysis Synthesis and Perception* (2nd edn). Springer.

Gurevich, M. I. 1965 *Theory of Jets in Ideal Fluids*. Academic.

Hirschberg, A. 1992 Some fluid dynamics of speech. *Bull. Commun. Parlee* **2**, 7–30.

Hofmans, G. C. J. 1998 Vortex sound in confined flows. PhD thesis, Eindhoven University of Technology.

Hofmans, G. C. J., Groot, G., Ranucci, M., Graziani, G. & Hirschberg, A. 2003 Unsteady flow through in-vitro models of the glottis. *J. Acoust. Soc. Am.* **113**, 1658–1675.

Howe, M. S. 1975 Contributions to the theory of aerodynamic sound, with application to excess jet noise and the theory of the flute. *J. Fluid Mech.* **71**, 625–673.

Howe, M. S. 1998 *Acoustics of Fluid–Structure Interactions*. Cambridge University Press.

Howe, M. S. 2003 *Theory of Vortex Sound*. Cambridge University Press.

Howe, M. S., Iida, M., Maeda, T. & Sakuma, Y. 2006 Rapid calculation of the compression wave generated by a train entering a tunnel with a vented hood. *J. Sound Vib.* **297**, 267–292.

Krane, M. H. & Wei, T. 2006 Theoretical assessment of unsteady aerodynamic effects in phonation. *J. Acoust. Soc. Am.* **120**, 1578–1588.

Landau, L. D. & Lifshitz, E. M. 1987 *Fluid Mechanics*, 2nd edn. Pergamon.

Lighthill, M. J. 1952 On sound generated aerodynamically. Part I: General theory. *Proc. R. Soc. Lond.* A **211**, 564–587.

Lighthill, J. 1978 *Waves in Fluids*. Cambridge University Press.

McGowan, R. S. 1988 An aeroacoustic approach to phonation. *J. Acoust. Soc. Am.* **83**, 696–704.

Mongeau, L., Franchek, C. H., Coker, C. H. & Kubli, R. A. 1997 Characteristics of a pulsating jet through a small modulated orifice, with application to voice production. *J. Acoust. Soc. Am.* **102**, 1121–1133.

Park, J. B. & Mongeau, L. 2007 Instantaneous orifice discharge coefficient of a physical, driven model of the human larynx. *J. Acoust. Soc. Am.* **121**, 442–455.

Rayleigh, Lord 1945 *Theory of Sound*, vol. 2. Dover.

Shadle, C. H., Barney, A. & Davies, P. O. A. L. 1999 Fluid flow in a dynamic mechanical model of the vocal folds and tract II: Implications for speech production studies. *J. Acoust. Soc. Am.* **105**, 456–466.

Stevens, K. N. 1998 *Acoustic Phonetics*. MIT Press, Cambridge, MA.

Teager, H. M. & Teager, S. M. 1983 The effect of separated air flow on vocalization. In (ed. I. R. Titze & R. C. Scherer, *Vocal Fold Physiology* (pp. 124–141). College-Hill, San Diego.

Zhang, Z., Mongeau, L. & Frankel, S. H. 2002 Experimental verification of the quasi-steady approximation for aerodynamic sound generation by pulsating jets in tubes. *J. Acoust. Soc. Am.* **112**, 1652–1663.

Zhao, W., Zhang, C., Frankel, S. H. & Mongeau, L. 2002 Computational aeroacoustics of phonation. Part I: Computational methods and sound generation mechanisms. *J. Acoust. Soc. Am.* **112**, 2134–2146.